Proceedings of the ASME 2017 36th International Conference on Ocean, Offshore and Arctic Engineering
OMAE2017
June 25-30, 2017, Trondheim, Norway

OMAE2017-61265

HYDRODYNAMICS OF FLEXIBLE PIPE WITH STAGGERED BUOYANCY ELEMENTS UNDERGOING VORTEX-INDUCED VIBRATIONS

Mengmeng Zhang
State Key Laboratory of Ocean Engineering,
Shanghai Jiao Tong University
Shanghai, 200030 China

Shixiao Fu[1]
State Key Laboratory of Ocean Engineering,
Shanghai Jiao Tong University
Shanghai, 200030 China

Leijian Song[2]
Marine Design & Research Institute of China
Shanghai 200011, China

SINTEF Ocean
Trondheim, Norway

Jie Wu
SINTEF Ocean
Trondheim, Norway

Halvor Lie
SINTEF Ocean
Trondheim, Norway

Haojie Ren
State Key Laboratory of Ocean Engineering,
Shanghai Jiao Tong University
Shanghai, 200030 China

ABSTRACT

Flexible riser with staggered buoyancy elements has been widely used in ocean engineering, such as steel lazy wave riser, drilling riser, etc. Both the buoyancy elements and the riser may experience vortex induced vibrations (VIV), subject to sea current. However, hydrodynamic characteristics of the buoyancy elements undergoing VIV and influence of buoyancy elements on hydrodynamic force of the bare section are still under discussion. The purpose of this paper is to reveal the hydrodynamic characteristics of flexible riser with staggered buoyancy elements, both for buoyancy element and bare pipe section. The cross flow hydrodynamic coefficients of the flexible riser with 25%, 50% and 100% staggered buoyancy covered are obtained from VIV model tests, using hydrodynamic forces and coefficients identification method. Distribution of the added mass coefficients and excitation coefficients along the flexible riser were investigated, and compared with those on the bare flexible pipe and rigid cylinders under forced oscillations. In addition, the relationship between added-mass coefficients of buoyancy element and that of bare section were obtained.

Keywords: buoyancy elements, flexible riser, vortex induced vibration, hydrodynamic force, added-mass coefficient, excitation coefficient

INTRODUCTION

Flexible riser with staggered buoyancy elements has been widely used in ocean engineering, such as steel lazy wave riser, drilling riser, etc. When VIV occurs, there is an interaction between vortex shedding from the bare pipe and the buoyancy element, which leads to complex hydrodynamic forces acting on the buoyancy element and the bare pipe segment.

There exist several model tests of flexible risers with staggered buoyancy elements performed at Marintek in a rotating rig or in a towing rig [1; 2; 3]. Also Li et al[4] presents experimental results from model tests with riser models with staggered buoyancy elements performed by SJTU SLOKE. Several metrics, the RMS amplitude ratio [2], frequencies of the peak spectral components [1; 4; 5] and the damping power at each excitation frequency[6] are proposed to determine the dominant excitation between bare

[1] Corresponding Author: Shixiao Fu, shixiao.fu@sintef.no, shixiao.fu@sjtu.edu.cn
[2] This co-author was a Ph.D. student in Shanghai Jiao Tong University.

and buoyancy elements of a pipe. Moreover, Rao [6]and Li [4]investigate the effect of buoyancy distribution on fatigue damage rate. Based on the test data, Wu [7]discussed the uncertainty and improvement of the VIV prediction software VIVANA. They found that the VIV response of riser with buoyancy elements is over-predicted, which is because the hydrodynamic force coefficients generalized from bare cylinder VIV tests may not be valid for cylinder with buoyancy elements. In order to predict VIV response of flexible pipe with buoyancy elements more accurately, more attention should be paid to the hydrodynamics of risers with buoyancy elements under VIV.

At present, researches on the hydrodynamics of riser have been focused on that of bare pipes (rigid or flexible) under VIV. Gopalkrishnan [8] and Aronsen [9] experimentally investigated the hydrodynamic forces on a cylinder under forced oscillation at purely CF and IL direction respectively. To systematically investigate into hydrodynamics of flexible riser under coupled VIV responses in IL and CF directions. Dahl [10] conducted two dimensional forced oscillation tests of rigid cylinder. Soni [11] and Yin and Larsen [12] studied vortex-induced force of flexible riser with realistic cross sectional orbits by forced oscillations of a smooth, rigid cylinder, where the oscillations replicated the motion at various cross-sections on a flexible riser as measured from flexible riser model tests. Wu et al. [13]obtained the vortex-induced forces and its coefficients on a flexible riser in the CF direction using an inverse method. Combining the modal analysis method and the Euler-Bernoulli beam vibration equations, Song et al. [14]analyzed the hydrodynamic force of a flexible riser using the strain information measured in the scaled model test.

The above analysis was focused on the hydrodynamic forces of the rigid and flexible bare pipes under VIV. In this paper, hydrodynamic forces and coefficients identification method was applied to obtain the hydrodynamic forces of the flexible riser with staggered buoyancy coverage of 25%, 50% and 100% from VIV model test of the flexible riser. Distribution of the added mass and exciting coefficients along the flexible pipe with staggered buoyancy were investigated, and compared with those on the bare and rigid cylinders under forced oscillations. The relationship between added-mass coefficient of buoyancy element and bare section was obtained. At last, the identified hydrodynamic coefficients were validated by ABAQUS.

HYDRODYNAMIC FORCE IDENTIFICATION

Hydrodynamic Forces

A submerged flexible riser with a tensional force T in a uniform current is illustrated in Fig. 1. The central axis of the riser lies on the x-axis. The direction of the flow is parallel to x-z plane and orthogonal to the riser.

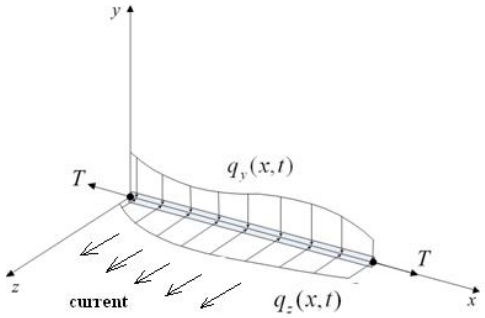

Fig. 1 Hydrodynamic forces of a submerged flexible riser with a tensional force in a current

According to FEM, the governing equation of spatial beam can be expressed as,

$$[M]\{\ddot{U}\}+[C]\{\dot{U}\}+[K]\{U\}=\{F\} \tag{1}$$

where M, C and K are global mass matrix, damping matrix and stiffness matrix of the riser, respectively and the detailed description can be found in Song[14]; $U,\dot{U},\ddot{U}$ are the displacement vector, velocity vector and acceleration vector respectively; F is the CF hydrodynamic force vector. The damping matrix C can be obtained based on Rayleigh damping model, and natural frequencies of the first and second dominant modes are applied to obtain parameters of Rayleigh damping model. Since only the hydrodynamic forces in CF direction is considered in this paper, the FEM model was simplified into a 3-degree of freedom model. The force vector, displacement vector, velocity vector and acceleration vector for one node can be expressed as:

$$\begin{aligned} F_i &= \{N_{xi} \quad N_{yi} \quad M_{zi}\}^T \\ U_i &= \{x_i \quad y_i \quad \theta_{zi}\}^T \\ \dot{U}_i &= \{\dot{x}_i \quad \dot{y}_i \quad \dot{\theta}_{zi}\}^T \\ \ddot{U}_i &= \{\ddot{x}_i \quad \ddot{y}_i \quad \ddot{\theta}_{zi}\}^T \end{aligned} \tag{2}$$

The VIV displacements y in CF direction can be obtained by modal superposition method from the corresponding bending strains[14].

With displacement vector U, the velocity vector $\dot{U}$ and acceleration vector $\ddot{U}$ can be obtained by the cubic-spline

difference method to calculate the first- and the second-order partial derivatives of U with respect to time.

After obtaining the structural response vectors $U, \dot{U}, \ddot{U}$, the hydrodynamic force F on the right side of Eq. (1) can be obtained by the inverse analysis.

Hydrodynamic coefficients

Assume that the vibration in the CF direction is composed of periodic vibrations with n different frequencies, the VIV displacement at node x can be expressed as

$$y(x,t) = \sum_{i=1}^{n} y_{0i}(x)\sin(\omega_i t + \theta_i) \tag{3}$$

where ω_i is the i^{th} frequency of vibration in the CF direction, $y_{0i}(x)$ and θ_i are the displacement amplitude and phase angle at frequency ω_i .

The VIV velocity $\dot{y}(x,t)$ and acceleration $\ddot{y}(x,t)$ can be obtained by differentiating Eq.(3):

$$\begin{aligned} \dot{y}(x,t) &= \sum_{i=1}^{n} y_{0i}(x)\omega_i \cos(\omega_i t + \theta_i) \\ \ddot{y}(x,t) &= -\sum_{i=1}^{n} y_{0i}(x)\omega_i^2 \sin(\omega_i t + \theta_i) \end{aligned} \tag{4}$$

The vortex-induced force at node x, $f_{CF}(x,t)$ can be written as

$$f_{CF}(x,t) = \sum_{i=1}^{n} f_{0i}(x)\sin(\omega_i t + \theta_i + \varphi_i) \tag{5}$$

where $f_{0i}(x)$ is the amplitude at frequency ω_i , and φ_i is the phase angle between the hydrodynamic force and the displacement at frequency ω_i .

Expanding the right side of Eq. (5),

$$\begin{aligned} f_{CF}(x,t) &= \sum_{i=1}^{n} f_{CF}(\omega_i, x, t) \\ &= \sum_{i=1}^{n} f_{0i}(x)\cos(\omega_i t + \theta_i)\sin(\varphi_i) \\ &\quad -(-f_{0i}(x)\sin(\omega_i t + \theta_i)\cos(\varphi_i)) \end{aligned} \tag{6}$$

Song pointed out that under a single frequency, the two terms in Eq. (6) are excitation force in phase with the velocity and added mass forces in phase with the acceleration respectively [8; 15; 14]; then the vortex induced forces of bare pipe segments and buoyancy segments under a single frequency can be expressed as:

$$f_{CF}(x,t) = f_{0i}(x)\cos(\omega_i t + \theta_i)\sin(\varphi_i) - (-f_{0i}(x)\sin(\omega_i t + \theta_i)\cos(\varphi_i))$$

$$\begin{cases} -\frac{1}{4}\rho\pi {D_{bare}}^2 l C_{a,bare}(x)\ddot{y}(x,t) + \frac{1}{2} D_{bare} l \rho U^2 C_{e,bare}(x)\frac{\dot{y}(x,t)}{y_{0i}(x)\omega} \\ \text{(on bare pipe)} \\ -\frac{1}{4}\rho\pi {D_{buoyancy}}^2 l C_{a,buoyancy}(x)\ddot{y}(x,t) + \frac{1}{2} D_{buoyancy} l \rho U^2 C_{e,buoyancy}(x)\frac{\dot{y}(x,t)}{y_0(x)\omega} \\ \text{(on buoyancy element)} \end{cases}$$

(7)

Where $C_{e,bare}(x), C_{e,buoyancy}(x)$ is the excitation coefficient at node x of bare segments and buoyancy elements respectively, $C_{a,bare}(x)$ and $C_{a,buoyancy}(x)$ is the added-mass coefficient at node x of bare pipe and buoyancy elements respectively, ρ is the fluid density, U is the fluid velocity, D_{bare} and $D_{buoyancy}$ are the diameter of the bare pipe and buoyancy elements respectively, and $y_{0i}(x)\omega$ is the amplitude of VIV velocity at node x.

Substituting Eq. (7) into Eq. (6), the vortex-induced forces under these multi frequencies can be expressed as the sum of hydrodynamic force under each single frequency:

$$f_{CF}(x,t) = \begin{cases} \sum_{i=1}^{n} \left(\frac{1}{2} D_{bare} l \rho U^2 C_{e,bare}(\omega_i, x)\frac{\dot{y}(\omega_i, x, t)}{y_{0i}(x)\omega_i} \right) \\ \quad \left(-\frac{1}{4}\rho\pi l {D_{bare}}^2 C_{a,bare}(\omega_i, x)\ddot{y}(\omega_i, x, t) \right) & \text{on bare pipe} \\ \sum_{i=1}^{n} \left(\frac{1}{2} D_{buoyancy} l \rho U^2 C_{e,buoyancy}(\omega_i, x)\frac{\dot{y}(\omega_i, x, t)}{y_{0i}(x)\omega_i} \right) \\ \quad \left(-\frac{1}{4}\rho\pi l {D_{buoyancy}}^2 C_{a,buoyancy}(\omega_i, x)\ddot{y}(\omega_i, x, t) \right) & \text{on buoyancy elements} \end{cases} \tag{8}$$

For staggered buoyancy pipes, there are two response frequencies and some non-linear interaction frequencies. The vortex-induced force and the VIV velocity and acceleration under each response frequency can be obtained by the band-pass filtering techniques. Then the excitation coefficient and the added-mass coefficient can be derived using the least squares method [16]. The reliability and biasless of this inverse method have already been validated by Song[16].

EXPERIMENTAL DESCRIPTION

A flexible riser model was towed in the towing tank of the Shanghai Shipping Science Institute to simulate a uniform flow [17; 4]. The riser model was horizontally placed in the tank. The two ends of the riser were connected to the towing carriage with universal joints. The towing carriage maintained constant pretension in the riser. A photograph of the experimental facility is shown in Fig. 2.

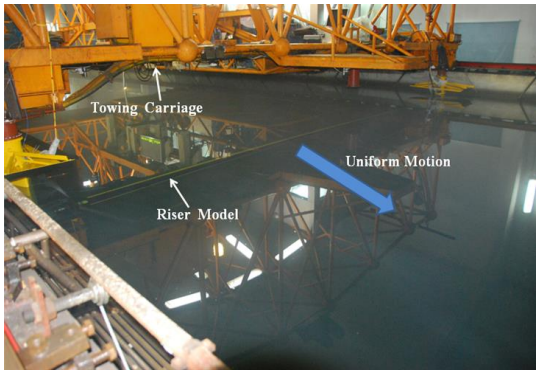

Fig. 2 Test facility for flexible riser in a uniform flow

The model parameters are listed in Tab. 1. The structural damping ratio 0.3% of bare pipe was obtained from a free-decay test of bare pipe in air. And it should be noted that the air damping is too small to neglect. It is known that the structural damping ratio is mainly influenced by materials. Fu pointed out that when the pipe was full covered by rubber (thickness of 5.6 D_{bare}), the damping properties of the pipe model didn't change much, which are 0.3% for bare pipe and 0.4% for pipe full covered by rubber [17]. The natural silica, as the main component of buoyancy module, has similar mechanical properties to rubber. Thus, the buoyancy elements can still be deemed to have little influence on the damping properties of the model, and 0.3% is adopted as the damping ratio of buoyancy elements approximately. The influences of this approximation on hydrodynamic coefficients have been discussed in the following section. And the results showed that this approximation has little influence on hydrodynamic coefficients of the model.

Tab. 1 Parameters of the riser model

Parameter	Units	Value
Total length between pinned ends	m	7.9
Bending stiffness, EI	$N.m^2$	1476.76
Young's modulus for pipe, E	N/m^2	1.08E11
Pretension	N	3000
Bare Pipe		
Outer diameter, D_R	mm	30
Mass in air	kg/m	1.768
Damping ratio	%	0.3
Buoyancy Element		
Outer diameter, D_B	mm	75
Length of each buoyancy element, L_B	m	0.3
Mass in air	kg/m	4.452

The main parameters that define the configuration of the buoyancy elements are illustrated in Figure 3 [3].

Three configurations are adopted in the experiment, including 25% coverage, 50% coverage and 100%. The buoyancy configurations are shown in Fig. 4 and the descriptions are as follows:

F01: 25% coverage condition: The length of the buoyancy accounted for 25% of the total riser length and the buoyancy elements were evenly spaced with gaps Lc of 0.9m.

F03: 50% coverage condition: The length of the buoyancy accounted for 50% of the total riser length. The buoyancy elements were not evenly spaced; the gaps Lc between buoyancy elements were 0.02m in the dense arrangement part and 0.9m in the sparse arrangement part.

F05: 100% coverage condition: The length of the buoyancy accounted for almost 100% of the total riser length. The buoyancy elements were evenly spaced with gaps Lc of 0.02m.

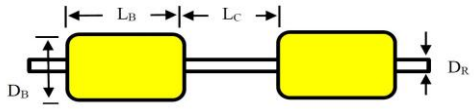

Fig.3 Definitions of L_C, L_B, D_R and D_B [3]

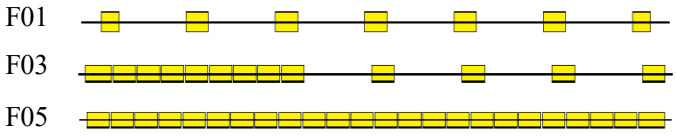

Fig.4 Configurations of buoyancy

A total of 88 Fiber Bragg grating (FBG) strain sensors were installed on the surface of the riser model in the CF and IL planes. The strain sensor was embedded into the fiber with the outer diameter at 125~ 140 μm and the fiber were then glued on the surface of the test riser model. There was a thin sleeve tube covered outside the test riser, the fiber, glue and sleeve tube were also considered in the physical characteristics of the test riser. Therefore, the FBG strain sensor would not affect the flow around the vibrating riser and the vibration characteristics of the flexible riser, and the FBG strain sensor was a mature technology which had been used in many VIV model tests of flexible riser[17].

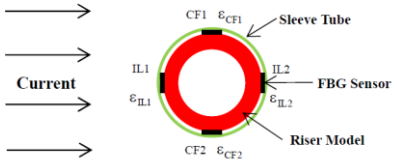

Fig.4 Arrangement of strain gauges on the surface of the riser model

The strain sensors were placed on opposite sides of a cross section at points denoted as CF1, CF2, IL1 and IL2, as shown in Fig. 4; the corresponding strains were denoted as ε_{CF1}, ε_{CF2}, ε_{IL1} and ε_{IL2}, respectively. The sensors were

installed at 19 cross sections in the CF plane (19 each at CF1 and CF2) and 25 cross sections in the IL plane (25 each at IL1 and IL2), and uniformly distributed in the CF and IL planes.

The strain sensors were recorded at a frequency of 250Hz. The strain signals from all the strain sensors were synchronously recorded. Thus, there was no phase lag between the strain signals at different measured locations along the riser.

RESULTS AND DISCUSSION

To investigate the characteristics of added mass coefficients and excitation force coefficients in CF direction, three riser configurations with buoyancy coverage of 25% (F01), 50% (F03) and 100% (F05) were selected with a current velocity of 1.6m/s and Vr_{bare} of 5.31 and 5.93 for F01 and F03 respectively, $Vr_{buoyancy}$ of 7.36 and 7.59 for F03 and F05 respectively. It should be noted that the reduced velocity are calculated based on the hydrodynamic diameter of bare riser and buoyancy, respectively.

$$Vr_{bare} = \frac{U}{f_{bare} \cdot D_{bare}} \tag{9}$$

$$Vr_{buoyancy} = \frac{U}{f_{buoyancy} \cdot D_{buoyancy}}$$

Where f_{bare} and f_{buoyancy} are vortex shedding frequencies of the bare pipe and buoyancy element; D_{bare} and D_{buoyancy} are hydrodynamic diameter of the bare pipe and buoyancy element.

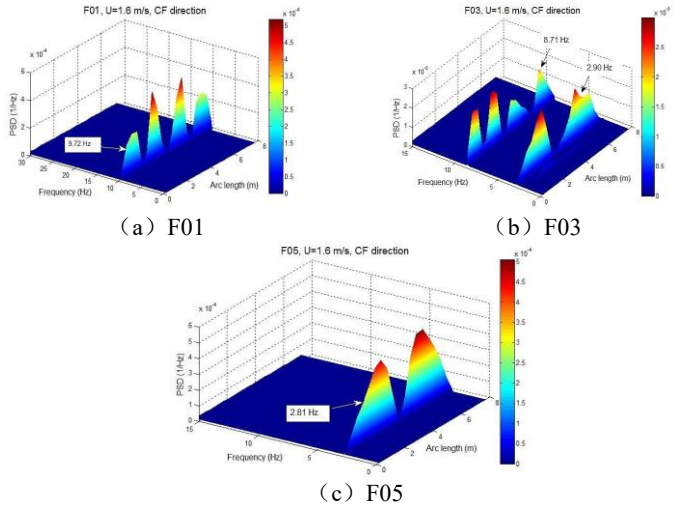

（a）F01　　（b）F03

（c）F05

Fig.5 Distribution of strain response along frequency and pipe (F01, F03, F05)

Riser response

The FFT analysis results of CF strain responses at 19 measured points are presented as Fig.5. It can be seen that for riser configuration F01 (25% coverage) and F05 (100% coverage), there is only one dominant response frequency; while for riser configuration F03, two dominant frequencies exist. The phenomenon of frequency varying under different buoyancy coverages is consistent with that of Li[4].

To obtain strain response under the dominant frequencies, band pass filtering was adopted. For F01, F03 and F05, the filter pass bands were 8.72 Hz ~ 10.72 Hz, 1.9 Hz ~3.9 Hz, 7.71 Hz ~9.71 Hz, and 1.81 Hz ~ 3.81 Hz respectively. Then, displacements in dominant frequencies are calculated by model analysis method.

Added mass coefficients

Based on displacement obtained above, hydrodynamic forces and coefficients of the riser are obtained by hydrodynamic forces and coefficients identification method. Fig. 6 to Fig. 9 presents the distributions of added mass coefficients and dimensionless displacement along the riser under conditions of 25% (F01), 50% (F03) and 100% (F05) buoyancy coverage.

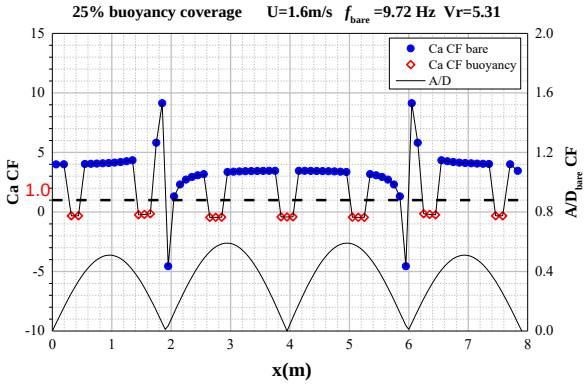

Fig.6 Distribution of added mass coefficients and dimensionless displacements along the riser under vortex shedding frequency of the bare pipe (F01)

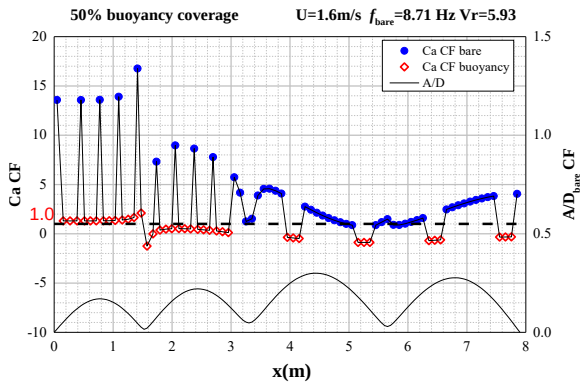

Fig.7 Distribution of added mass coefficients and dimensionless displacements along the riser under vortex

shedding frequency of the bare pipe (F03)

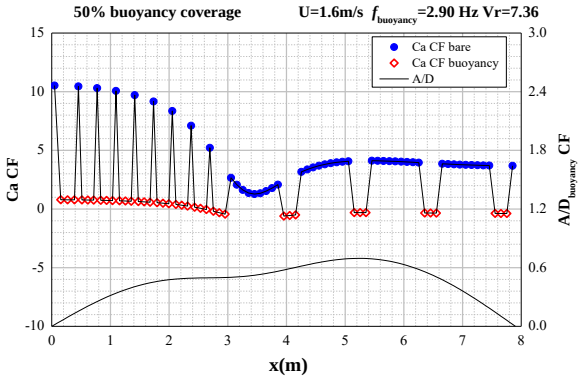

Fig.8 Distribution of added mass coefficients and dimensionless displacements along the riser under vortex shedding frequency of the buoyancy element (F03)

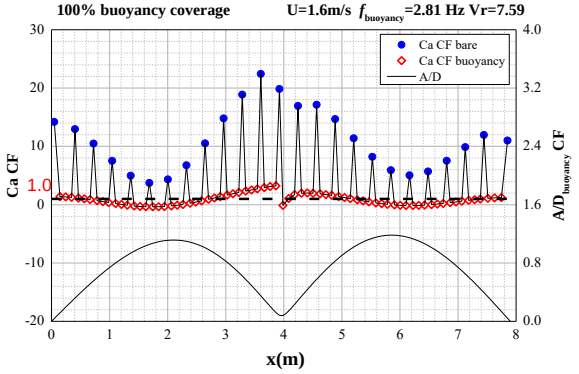

Fig.9 Distribution of added mass coefficients and dimensionless displacements along the riser under vortex shedding frequency of the buoyancy element (F05)

From Fig. 6 to Fig. 9, it can be found that the added mass coefficient on the flexible riser with buoyancy elements has a 'jagged' distribution along the riser. The added mass coefficient on the bare pipe is much larger than that on the buoyancy elements, and varies with different gaps between adjacent buoyancies. Under the condition of spacing ratio Lc/L_B = 3/1 (F01 and the sparse part of F03), the added mass coefficient at the bare pipe section varies between 1.0 and 4.5, while are always in negative values on the buoyancy elements varying between -1 to 0. When spacing ratio Lc/L_B = 0.07/1 (F05 and the dense part of F03), the added mass coefficient at the bare pipe is much greater than 1.0, which varies between 3.7 and 22. While the added mass coefficient of the buoyancy element is in the range of -0.37 to 3.2, which is basically the same as that in the traditional frequency domain prediction.

The explanation of this phenomenon could be that when the riser with buoyancy element experiencing VIV, the water between two adjacent buoyancy elements is trapped and forced to move together with the buoyancy elements, leading to that the bare pipe between these two buoyancy elements will be surrounded by a large volume of water. Based on this assumption, the added mass coefficients distribution of F05 (spacing ratio of 0.07) may result from that under the buoyancy response frequency, the bare pipe bounded with a large volume of water is forced to oscillate as a virtual buoyancy element, as shown in Fig. 10(a). Thus when the added mass coefficients of buoyancy module is of 0.0 - 2.0 (with respect to the volume of the buoyancy module), then by simple calculation it can be found that the added mass coefficient with respect to the volume of the bare pipe will be in the range of 3 to 25, which is quite similar with present results. Then with the increase of gap between two adjacent buoyancy elements, only part of the water between the buoyancy elements may be trapped. For the spacing ratio Lc/L_B of 3/1, by calculation from the identified added mass coefficients of the bare pipe, around 60% of the water was trapped and forced to oscillate with the bare pipe. In addition, for the spacing ratio Lc/L_B of 3/1, the dominant frequency is the vortex shedding frequency of the bare pipe. It means that the buoyancy element would be forced to oscillate as the virtual bare pipe and the corresponding added mass coefficient with respect to the volume of the buoyancy element is -0.33, which is similar with the identified results.

The above analysis indicates that under different spacing ratios, values of the added mass coefficients will be much different. However, the accurate conclusion on the influence of spacing ratio cannot be obtained due to the limited riser configurations in this paper. Further experiment should be conducted by varying different spacing ratio.

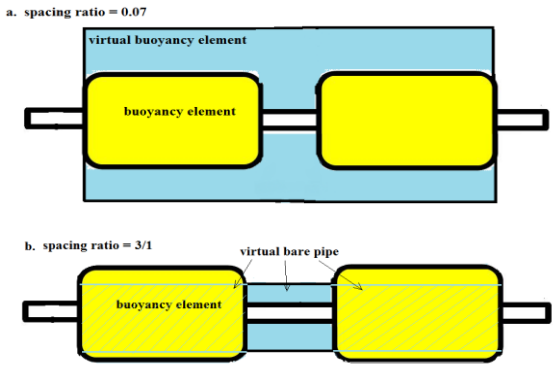

Fig. 10 scheme of virtual buoyancy and bare pipe

In this paper, we try to obtain the relationship between added mass coefficients of bare pipe and buoyancy element, by keeping the spacing ratio constant. The total mass of the riser (including the structural mass and the added mass) and the total mass force are extracted for analysis. The added

mass m_a is defined as:

$$m_a = C_a \cdot \frac{1}{4}\rho\pi D^2 \tag{10}$$

Where C_a is the added mass coefficient, ρ is water density and D is the hydrodynamic diameter of the riser. D_{bare}=0.031 m and $D_{buoyancy}$=0.075 m are used in the calculation of added mass at bare pipe and buoyancy element, respectively.

Then the total mass m is defined as the sum of added mass and the structural mass:

$$m = m_a + m_s \tag{11}$$

Similarly, the total mass force is defined as the sum of inertia force of the structural F_i and F_{am}:

$$F_{m\,total} = F_i + F_{am} = m_s \cdot a + m_a \cdot a = (m_s + m_a) \cdot a \tag{12}$$

Where F_i is the structural inertia force that equals the product of structural mass m_s and acceleration a; F_{am} is the added mass force that equals the product of added mass m_a and acceleration a.

Fig.11 presents the distribution of added mass coefficient, non-dimensional vibration amplitude, added mass, structural mass, total mass of vibration and the RMS value of total mass force in CF direction along the riser of F01. It shows that when VIV of the riser covered with buoyancy elements occurs, the total mass and total mass force of buoyancy elements are consistent with those of bare pipes along the riser. However, the buoyancy elements and bare pipe section are different in structural mass, as shown in Fig. 11(c), structural mass of buoyancy elements and bare pipe are 6.22kg/m and 1.768kg/m, respectively. It can be found that the difference between buoyancy elements and the bare pipe in added mass compensate their difference in structural mass, which leads to a consistent total mass distribution along the whole riser. Based on this, the relationship between buoyancy elements and the bare pipe in total mass can be expressed as:

$$(m_s + m_a)_{bare} = (m_s + m_a)_{bouyancy} \tag{13}$$

And the non-dimensional total mass of riser is defined as

$$m^*_{bare} = \frac{(m_s + m_a)_{bare}}{\pi D^2_{bare}\rho/4}$$
$$m^*_{buoyancy} = \frac{(m_s + m_a)_{buoyancy}}{\pi D^2_{buoyancy}\rho/4} \tag{14}$$

The ratio between the total mass of bare pipe and buoyancy elements can be obtained by combining equation (13) and (14):

$$\frac{m^*_{buoyancy}}{m^*_{bare}} = \frac{(m^*_s + C_a)_{buoyancy}}{(m^*_s + C_a)_{bare}} = \left(\frac{D_{bare}}{D_{bouyancy}}\right)^2 \tag{15}$$

where m^*_s is the structural mass ratio. This relationship can realize the transformation between the added mass in buoyancy and bare riser, and only one added mass coefficient of bare riser or buoyancy need to be determined in predicting VIV response frequencies of flexible riser that covered buoyancy blocks.

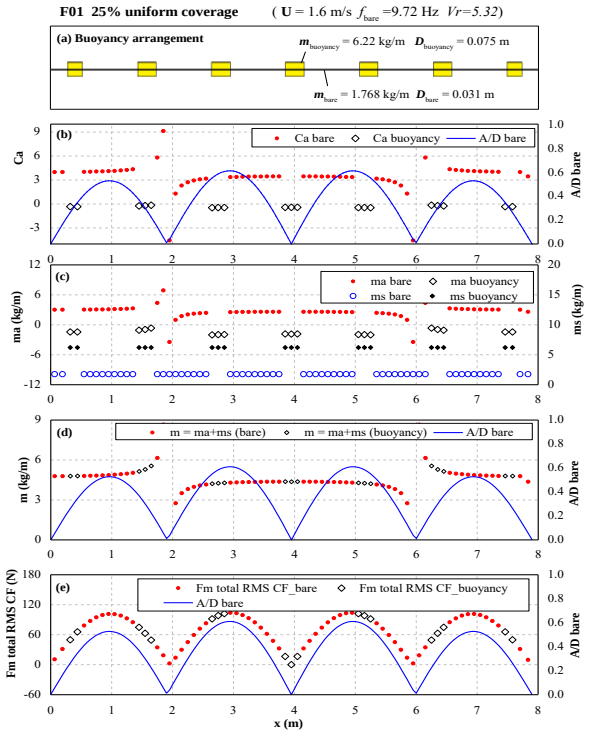

Fig. 11 Distribution of added mass coefficients, added mass, structural mass, total mass and total mass force in CF direction along the riser (F01)

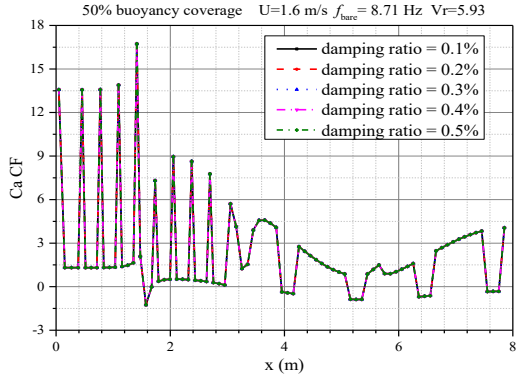

Fig.12 Added mass coefficients distributions under different damping ratios for F03

As mentioned above, the damping ratio of buoyancy elements covered model (F01, F03 and F05) is taken as the same as that of the bare pipe approximately. To validate the biases of the damping ratios used, the sensitivity of damping ratios on added mass coefficients is discussed. Five damping ratios ranging from 0.1% to 0.5% are selected. The identified added mass coefficients of F03 under bare response frequency are presented in Fig. 12. It can be found that the change of the damping ratio has no effect on the added mass coefficients of bare pipe and buoyancy elements. It is feasible to approximate the damping ratio of buoyancy elements with value of 0.3%.

To further validate the identified added mass coefficients, FEM model of the riser is built based on the riser parameters in Tab. 1. Then, the natural frequencies that correspond to the dominant mode in CF direction are computed using the added mass coefficient by the finite element model. The comparison of the calculated frequencies and the measured dominant frequencies for different riser configures is shown in Tab.2. It can be seen that there is a very good agreement between the calculated and measured frequencies, which verified the accuracy of identified added mass coefficients.

Tab. 2 Comparison of the calculated and measured dominant frequencies

	F01	F03(f_{bare})	F03($f_{buoyancy}$)	F05
Measured （Hz）	9.72	8.71	2.90	2.81
Calculated （Hz）	9.72	8.74	3.10	2.82
Relative error （%）	0.01	0.46	6.89	0.16

It should be noted that sudden changes of added mass coefficients occurred at nodes of vibration (in Fig. 6) is primarily due to numerical errors for small response amplitudes at nodes [16; 20]. The sudden change of the added mass coefficients may lead to unreasonable minus total mass in the predication of VIV response frequencies and has been deleted in the frequency calculations.

Excitation coefficients

Fig. 13 to Fig.15 illustrate the distribution of excitation coefficients in CF direction along the flexible riser corresponding to riser configurations of F01, F03 and F05. It can be seen that the excitation coefficients have a 'jagged' distribution along the riser, and have a larger value on the bare pipe than on the buoyancy element. Moreover, the exciting coefficients shown in Fig.14-15 present the same "varying modes" as those on the displacement and are in a parabola shape between two vibration nodes with clear peak/bottom ranges.

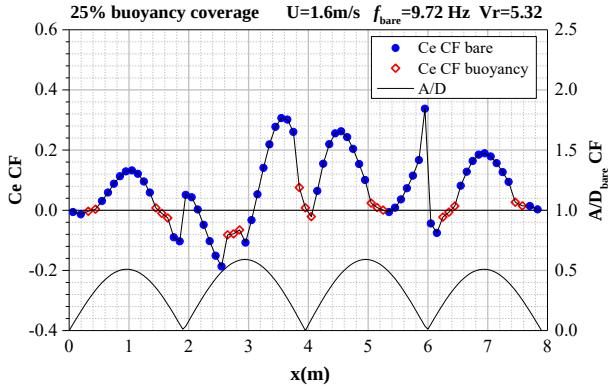

Fig.13 Distribution of excitation coefficients and non-dimensional displacement along the riser (F01)

As shown in Fig.13, for riser configurations of buoyancy coverage of 25% (F01), the excitation coefficients in bare pipe and buoyancy element varies between -0.2 to 0.33 and -0.08 to 0.08, respectively. It is interesting to find that the ratio between these two varying ranges are much close to 2.5, equal to the diameter ratio ($D_{buoyancy}/D_{bare}$=2.5). Additionally, based on the semi-empirical frequency-domain VIV prediction theory ([19] [18]) based on the forced-oscillation test of a rigid cylinder, under vortex shedding frequency of bare pipe (shown in Fig.13), the reduced velocity of bare pipe is 5.32; the bare pipe should be in the excitation region with positive excitation coefficients. While the reduced velocity of buoyancy element is 2.128, the buoyancy elements should serve as a damper with negative coefficients. However, some of the excitation coefficients in Fig. 13 are negative on bare pipe and positive on buoyancy elements. This discrepancy has already been found by Song [16]. That is the excitation coefficients were negative in certain intervals for bare riser under uniform flow with reduced velocity of 7.21 and 5.38. The primary reason for the phenomenon is that the phase angles between CF and IL VIV displacements were not equal in certain regions, which leads to various vortex shedding modes at certain locations on the riser [12]. Consequently, the hydrodynamics for VIV were different. Besides, flow field around the bare pipe and buoyancy elements are mutually affected, which further leads to the certain damping region of bare pipe and excitation region of buoyancy elements.

The excitation coefficients distributions of F03 are shown in Fig.14. It can be seen that under the buoyancy response frequency 2.90 Hz, the magnitudes of excitation coefficients vary from -0.17 to 0.33 for buoyancy elements, and from -0.43 to 0.81 for bare pipe. Under the bare response frequency 8.71 Hz, the excitation coefficients vary from -0.16 to 0.12 for buoyancy elements, and from -0.36 to 0.36 for bare pipe which is a little smaller than those under the

buoyancy response frequency. A smaller value of excitation coefficients leads to a smaller displacement response under bare response frequency, as shown in Fig.6. Besides, the ratios between excitation coefficients variation ranges on bare pipe and buoyancy elements are close to the diameter ratio 2.5, which is similar as the phenomenon for F01.

Moreover, under the buoyancy response frequency of F03 riser configuration (Fig.14 (a)), the excitation coefficients are always positive for the buoyancy element and bare pipe both in the densely covered part (from 0 to 3m), while are mostly negative in the sparsely covered part (from 3m to 7.9m). It clearly showed that the excitation coefficients on the sparsely covered part, around 10 $D_{buoyancy}$ long, nearby the buoyancy densely covered part are strongly affected by the neighboring buoyancy densely covered parts, and locates in the exciting region with positive excitation coefficients. The similar distribution trends can also be found for the riser under bare response frequency as illustrated in Fig.14 (b).

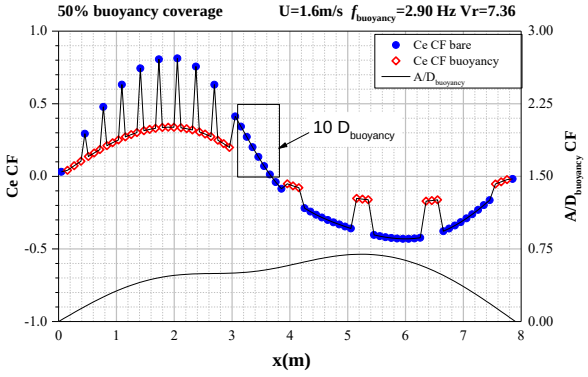

(a) under buoyancy response frequency

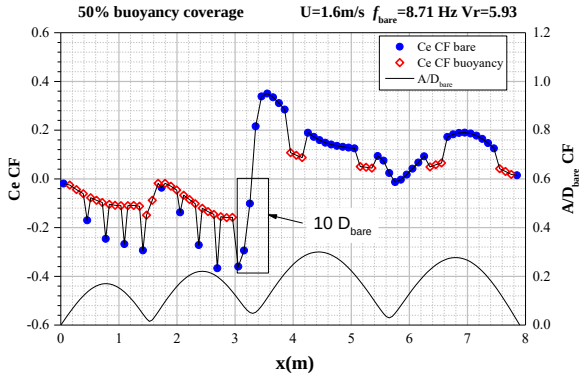

(b) under bare response frequency

Fig.14 Distribution of excitation coefficients and non-dimensional displacement along the riser (F03)

Fig. 15 presents the distribution of excitation coefficients and non-dimensional displacement A/$D_{buoyancy}$ along the riser for F05 (100% buoyancy covered). The magnitudes of the excitation coefficients for F05 are in the range of -0.28 to 0.42 for the buoyancy elements, and -0.75 to 1.03 for bare pipe. The ratio of these two variation ranges is very close to the ratio of their outer diameters 2.5 ($D_{buoyancy}$/D_{bare}).

Besides, the excitation coefficients on the bare parts and buoyancy parts presented in Fig.13-15 are always in the same sign (positive or negative). This phenomenon may result from the fact that the flexible riser with buoyancy elements experiences a more evident three dimensional flow field when VIV occurs, and hydrodynamic loads of the bare pipe and buoyancy elements are affected by each other.

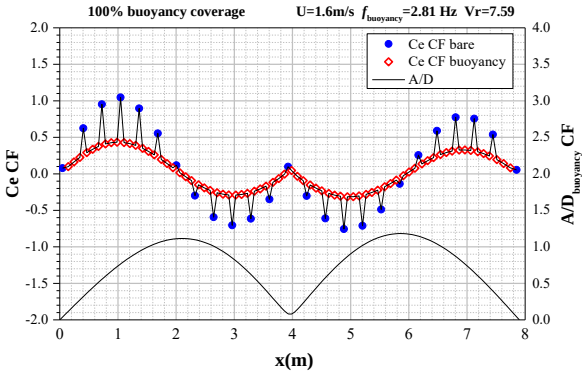

Fig.15 Distribution of excitation coefficients and non-dimensional displacement along the riser (F05)

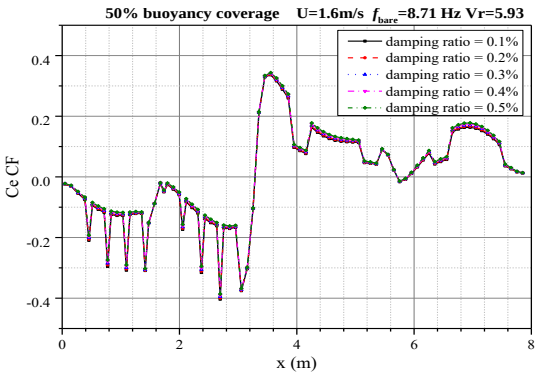

Fig.16 Distribution of excitation coefficients along the riser under different damping ratios for F03

In order to verify the influences of the damping ratio approximation on excitation coefficients, the sensitivity of damping ratios on excitation coefficients is discussed. As shown in Fig.16, excitation coefficients under five damping ratios, which range from 0.1% to 0.5%, are much close. The maximum difference is less than 5%. This indicates that the approximation has little influence on excitation coefficients of the model.

To investigate the difference in the excitation coefficients between the flexible riser with staggered buoyancy element and the forced oscillation rigid cylinder directly, the variation of CF excitation coefficients with the non-dimensional displacement under conditions of F01 are shown in Figs. 17. It can be found that the excitation

coefficients identified in this paper are different from those obtained in purely CF forced oscillation test of rigid cylinder. For a certain reduced velocity and non-dimensional displacement, there would be one excitation coefficient according to the results of Gopalkrishnan[8]. However, it is very interesting to find that there are several identified excitation coefficients under a certain reduced velocity and non-dimensional displacement. Besides, at a certain reduced velocity, there are several trends of excitation coefficients under the increase of non-dimensional displacement. For instance, In Fig.17, the CF excitation coefficient obtained by Gopalkrishnan increases from -0.28 to 0.35 with the non-dimensional displacement increasing from 0.23 to 0.5, and then decreases to 0.12 with non-dimensional displacement increasing to 0.6. While the CF excitation coefficients identified in this paper shows three completely different varying trends. The discrepancy indicates that aside from reduced velocity and non-dimensional displacement, there are other influence factors of excitation coefficients for pipes with staggered buoyancy, such as the phase angle between the CF and IL VIV displacements [13], the amplitude of IL displacements, and Reynolds number and so on. Further investigations of the influence factors should be carried out.

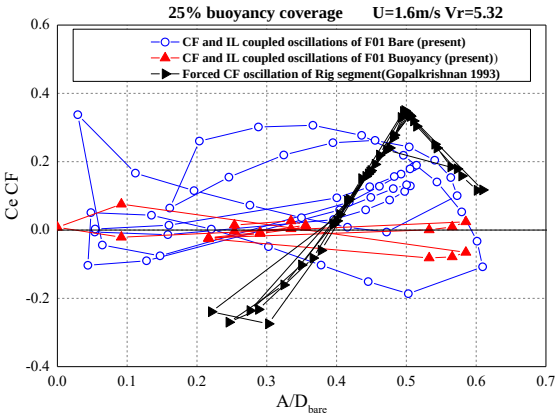

Fig.17 CF excitation coefficients vs. non-dimensional response amplitude (Vr =5.32 for F01)

To test the validity of the identified hydrodynamic forces and force coefficients, the vortex-induced forces were reconstructed using Eq. (8). Based on the reconstructed vortex-induced force, the strain response was obtained using the finite element analysis conducted by ABAQUS. Fig. 18 shows the measured and calculated axial distributions of the RMS values for the strains. As can be observed in the figure, the calculated values for riser configuration of F01, F03 and F05 agree well with the measured values. This consistency in the results demonstrates the validity of the identified hydrodynamic forces and force coefficients in this paper.

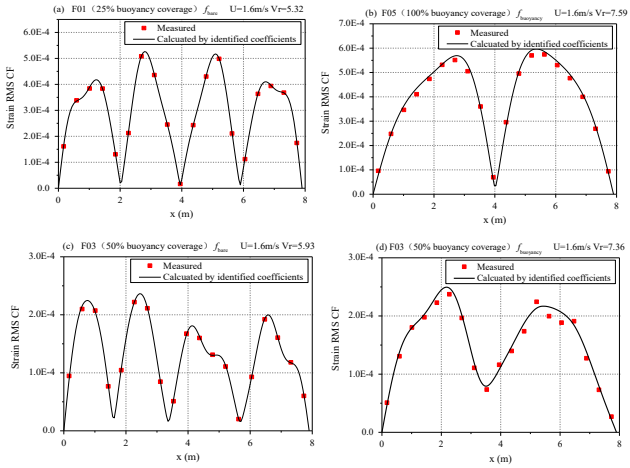

Fig.18 axial distributions of the RMS values of the measured and calculated strains (F01, F03 and F05)

CONCLUSION

To reveal the hydrodynamic characteristics of flexible riser with staggered buoyancy module, the hydrodynamic coefficients of the flexible riser with 25%, 50% and 100% buoyancy covered are obtained from VIV model test of the risers, using hydrodynamic force and coefficients identification method. The added-mass coefficient and excitation coefficient in CF direction of the bare pipe and the buoyancy element for different buoyancy coverage were investigated. Moreover, similarities and differences between the hydrodynamic coefficients identified in this paper and the existing database used in VIV prediction were discussed. Lastly, the hydrodynamic coefficients identified in this paper were verified by FEM using ABAQUS. The following conclusions can be drawn:

1) The added-mass coefficients of bare pipe are relatively larger than those of buoyancy module. And a smaller gap between two adjacent buoyancy elements will lead to a larger added-mass coefficient of bare section. Values of the added mass coefficient on bare pipe and buoyancy elements will be affected by spacing ratios, mass ratios and diameter ratio. Also, more investigations need to be conducted on the influence of these factors.

2) On a flexible pipe with staggered buoyancy module, when the added mass coefficient on bare pipe or buoyancy element is already known, added mass coefficient on the other one can be obtained by the relationship between added-mass coefficients, diameter ratio and mass ratio on buoyancy element and bare section.

3) Under condition of 25% and 50% buoyancy coverage, the range of excitation coefficient Ce on the buoyancy elements is much smaller than that on the bare section. And the ratio

of excitation coefficient between buoyancy module and bare pipe is equal to the reciprocal of diameter ratio 2.5.

4) There are some differences between excitation coefficients identified in this paper and the existing database used in the semi-empirical prediction theory, especially in the existing multi values of excitation coefficients under a certain A/D and reduced velocity. More studies on these differences should be conducted.

ACKNOWLEDGMENTS

This research was supported by the National Natural Science Foundation of China under Grant Number 51490674 and 51490675.

REFERENCES

[1] Jhingran, V., Zhang, H., Lie, H., Braaten, H., & Vandiver, J. (2012). Buoyancy Spacing Implications for Fatigue Damage due to Vortex-Induced Vibrations on a Steel Lazy Wave Riser (SLWR). OTC 2012.Houston, Texas, USA.

[2] Lie, H., Mo, K., & Vandiver, J. (1998). VIV Model Test of a Bare and a Staggered Buoyancy Riser in a Rotating Rig. OTC 1998.Houston, Texas, USA.

[3] Wu, J., Lie, H., Constantinides, Y., & Baarholm, R. J. (2016). NDP Riser VIV Model Test With Staggered Buoyancy Elements.ASME 2016 International Conference on Ocean, Offshore and Arctic Engineering, Busan, South Korea.

[4] Li, L., Fu, S., Yang, J., Ren, T., & Wang, X. (2011). Experimental Investigation on Vortex-Induced Vibration of Risers With Staggered Buoyancy.ASME 2011 International Conference on Ocean, Offshore and Arctic Engineering, Rotterdam, The Netherlands.

[5] Vandiver, J., & Peoples, W. (2003). The Effect of Staggered Buoyancy Modules on Flow-Induced Vibration of Marine Risers. OTC 2003.Houston, Texas, USA.

[6] Rao, Z., Vandiver, J. K., & Jhingran, V. (2015). Vortex induced vibration excitation competition between bare and buoyant segments of flexible cylinders. Ocean Engineering, 94, 186-198.

[7] Wu, J., Lekkala, M. R., & Ong, M. C. (2016). Prediction of Riser VIV With Staggered Buoyancy Elements.ASME 2016 International Conference on Ocean, Offshore and Arctic Engineering, Busan, South Korea.

[8] Gopalkrishnan, R. (1993). Vortex-induced forces on oscillating bluff cylinders. Ph. D thesis, Massachusetts Institute of Technology, Cambridge, MA, USA.

[9] Aronsen, K. H. (2007). An Experimental Investigation of In-line and Combined In-line and Cross-flow Vortex Induced Vibrations. Ph. D Thesis, NTNU, Trondheim, Norway.

[10] Dahl, J. (2008). Vortex-induced vibration of a circular cylinder with combined in-line and cross-flow motion. Ph. D thesis, Massachusetts Institute of Technology, Cambridge, MA, USA.

[11] Soni, P. K. (2008). Hydrodynamic Coeffcients for Vortex-Induced Vibrationsof Flexible Beams. Ph. D thesis, NTNU, Trondheim, Norway.

[12] Yin, D., & Larsen, C. M. (2011). Experimental and Numerical Analysis of Forced Motion of a Circular Cylinder.ASME 2011 International Conference on Ocean, Offshore and Arctic Engineering, Rotterdam, The Netherlands.

[13] Wu, J., Lie, H., Larsen, C. M., Liapis, S., & Baarholm, R. (2016). Vortex-induced vibration of a flexible cylinder: Interaction of the in-line and cross-flow responses. Journal of Fluids & Structures, 63, 238-258.

[14] Song, L., Fu, S., Zeng, Y., & Chen, Y. (2016). Hydrodynamic Forces and Coefficients on Flexible Risers Undergoing Vortex-Induced Vibrations in Uniform Flow. Journal of Waterway Port Coastal & Ocean Engineering, 142(4), 4016001.

[15] Sarpkaya, T. (1977). Transverse oscillations of a circular cylinder in uniform flow, part 1. Monterey, CA, USA.: Naval Postgraduate School.

[16] Song, L., Fu, S., Cao, J., Ma, L., & Wu, J. (2016). An investigation into the hydrodynamics of a flexible riser undergoing vortex-induced vibration. Journal of Fluids & Structures, 63, 325-350.

[17] Fu, S., Ren, T., Li, R., & Wang, X. (2011). Experimental Investigation on VIV of the Flexible Model Under Full Scale Re Number.ASME 2011 International Conference on Ocean, Offshore and Arctic Engineering, Rotterdam, The Netherlands.

[18] Vandiver, J. K. (2003). SHEAR7 User Guide 4.5. Department of Ocean Engineering, Massachusetts Institute of Technology, Cambridge, MA, USA.

[19] Larsen, C. M., Yttervik, R., Passano, E., & Vikestad, K. (2001). VIVANA Theory Manual. Version 3.1. Trondheim, Norway.

[20] Wu, J. (2011). Hydrodynamic Force Identication from Stochastic Vortex Induced Vibration Experiments with Slender Beams. Ph. D thesis, NTNU, Trondheim, Norway.